Conformation of Polymer Brushes under Shear: Chain Tilting and Stretching

Ling Miao,* Hong Guo, and Martin J. Zuckermann

Centre for the Physics of Materials, Department of Physics, McGill University, Montréal, Québec, Canada H3A 2T8

Received July 24, 1995; Revised Manuscript Received November 3, 1995[⊗]

ABSTRACT: We have studied the conformation of a polymer brush in equilibrium with a solvent that is subject to a shear flow. The interplay between the polymer brush and the hydrodynamic flow of the solvent has been modeled, with simple but largely justifiable approximations. The main technique used in our study is a Monte-Carlo simulation algorithm that is distinct from many standard numerical methods used in studies of polymer brushes in that it combines an off-lattice description of polymer brushes—the Edwards Hamiltonian—with a modification of the standard Metropolis Monte-Carlo transition probability to take into account the effective force acting upon the polymer molecules by the moving solvent. The conformation of the polymer brush, the configurations of each individual chain in particular, is investigated in detail. It is found that the significant response of the brush to the solvent shear flow manifests principally in the form of the chain tilting toward and stretching along the direction of the flow, whereas the overall conformational properties, such as the averaged local monomer density, and the linear span of the brush in the direction normal to that of the flow remain essentially unaffected by the flow. Such response can be understood both qualitatively and semiquantitatively in terms of a notion of the mechanical balance of the different physical forces involved, which was used in the theory of Rabin and Alexander (Rabin, Y.; Alexander, S. *Europhys. Lett.* **1990**, *13*, 49). The relevance of our study to some recent experiments is briefly discussed.

1. Introduction

Polymer brushes form when long-chain polymer molecules are grafted by one end on a surface or interface, with a grafting density high enough so that the chains are forced to stretch away form the surface. They are a central model in many important problems in polymer science, such as the stabilization of colloidal dispersions,[1] lubrication of surfaces, and adhesion.[2]

Configurations of the long molecules in a brush depend crucially on whether solvent is present or absent (as in cases of polymer melts) and also, if solvent is present, on the affinity of the polymer to the solvent (good or poor solvent). In this paper, we concentrate on the case where polymer brushes are exposed to a good solvent. In this situation the basic physics governing the static behavior of brushes are well understood, as demonstrated by the agreement between the mean-field scaling arguments,[3] self-consistent field calculations,[4] computer simulations,[5,6] and experiments[7] (see also ref 8, for recent reviews). A polymer molecule dispersed in a good solvent has two opposite tendencies: one, to maximize its configurational entropy by adopting random-walk configurations; the other, to be wet as much as possible by the solvent (or the excluded-volume effect). In a semidilute solution of free polymer molecules of length N (measured in units of the persistence length, b), the entropy dominates and the linear extension of the molecules is characterized by the radius of gyration, R_g, which scales as $N^{1/2}b$. A rather different situation appears when such chains are grafted to a solid surface at a density of σ chains per unit area, where $\sigma^{-1/2}$ is much smaller than R_g: The entropic effect weakens, for the configurational entropy has to be sacrificed for the chains to avoid contact with each other. The result of the competition between the two effects leads to a brush formed by stretched chains which have little overlap with its neighboring chains. The equilibrium brush height, a measure of the linear extension of the molecules in the brush, scales as $N\sigma^{1/3}$, clearly indicating that the chains are stretched far beyond their dimension in free solution. However, it is also important to keep in mind that coiling on a shorter length scale (a few persistence lengths) is still inherent in the conformation of these stretched chains, since their linear span is still much smaller than their fully-extended length. Figure 1a illustrates such a molecular conformation.

Studies that would answer the question of how a brush with the static properties described in the previous paragraph responds to *macroscopic* flow of the solvent are easily motivated, as solvent flow is often involved in many applications of polymer brushes. Recently, experiments have been performed to measure the response of sheared polymer brushes.[9] On the other hand, theoretical studies of such dynamic aspects of polymer brushes have so far been rather limited.[10,11] In any such study, in addition to the issue of how to deal with the large number of degrees of freedom involved in these systems, at least two other questions have to be addressed. (1) What effects does a macroscopic flow of the solvent have on the microscopic motion of polymer molecules? (2) How do the presence and the dynamic behavior of a polymer brush influence the flow of the solvent?

It is the purpose of this paper to study by means of a Monte-Carlo (MC) simulation the properties of a polymer brush under shear, in particular the configurations of the long molecules in the brush. In dealing with the large number of degrees of freedom, we built our simulation on an off-lattice Monte-Carlo simulation algorithm which was developed by Laradji *et al.*[6] to study the equilibrium properties of polymer brushes. The algorithm uses the same Hamiltonian as that used in SCF theory[4] to describe the microscopic configurations of a brush and has been tested to satisfaction in the context of equilibrium theory for polymer brushes for a wide range of chain lengths and grafting densities.

[⊗] Abstract published in *Advance ACS Abstracts,* February 15, 1996.

0024-9297/96/2229-2289$12.00/0

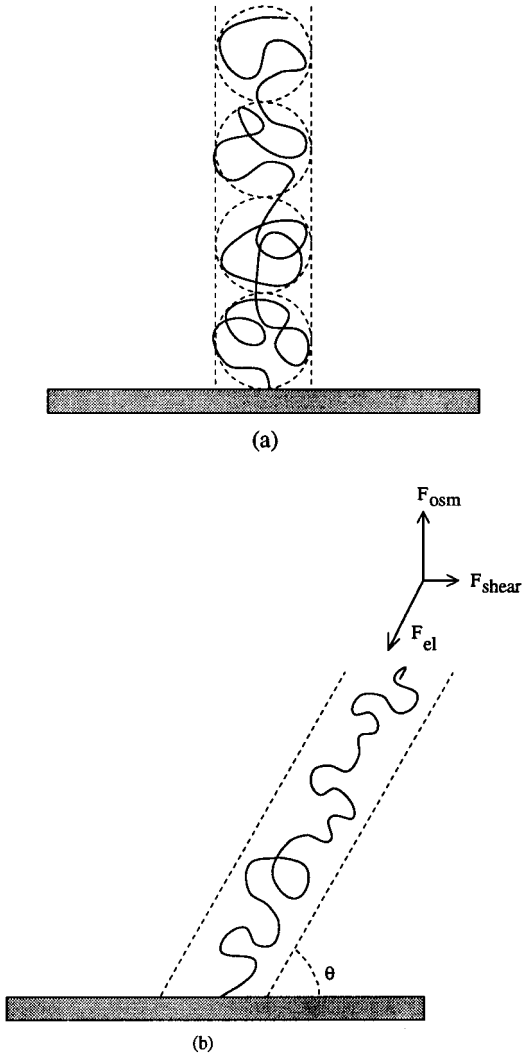

Figure 1. Schematic picture of the conformation of polymer chains in a brush. (a) In equilibrium: The chain is stretched but also has substantial local coiling represented by the "blobs". (b) Under shear: The chain is tilted, and the local coiling is reduced due to further stretching by the shear force. θ is the angle of tilting; the balance of the osmotic pressure, the elastic restoring force, and the shear force is also illustrated.

Detailed information on the brush, including the effect of fluctuations,[12] is the natural outcome of the simulations. Furthermore, the off-lattice nature of our algorithm makes the computation very efficient for large systems of long-chain molecules, and the algorithm should be a rather powerful one, especially when large-size (scaling) behavior of polymer systems is at issue.

The effect of macroscopic flow of the solvent on the microscopic motion of polymer molecules is phenomenologically represented by asymmetric jumping rates for monomers: The jumping rate in the direction of the flow is higher than that against the flow, and the difference is proportional to the local velocity of the flow. This was originally used by Katz *et al.* in MC studies of driven lattice gases[13] and later applied by Lai and Binder[11] in a study of polymer brushes under shear that our work is similar to. The physics underlying this idea are intuitively simple. Consider a Brownian particle that is in a fluid and has a macroscopic velocity, $\vec{v}$, relative to the fluid; the averaged force acting on the Brownian particle by the fluid should be $-\zeta\vec{v}$, where ζ is the friction coefficient for the particle. In our Monte-Carlo procedure, the effect of this force is translated into an enhanced jumping rate in the flow direction.

The hydrodynamic interaction between monomers[14-16] has been effectively neglected when we use the Edwards Hamiltonian to describe the brush configurations. This approximation may be justified when relatively dense brushes are being considered. In these cases, the monomer density is significant enough to effectively increase the macroscopic (over length scales of order $\sigma^{-1/2}$) viscosity of the solution, thereby diminishing the strength of the hydrodynamic interaction beyond a certain length scale (often referred to in literature as "hydrodynamic screening length") and making it effectively a short-range interaction.[16-18]

To address in terms of a first-principles treatment the second question, namely, the interplay between the dynamic behavior of a polymer brush and the hydrodynamics of its solvent, is quite a formidable task. We therefore take a phenomenological approach to this issue, as Milner has suggested,[19] which invokes the Brinkman equation[20] to describe the flow field of the solvent inside the brush region:

$$\rho\left(\frac{\partial\vec{v}}{\partial t} + \vec{v}\cdot\vec{\nabla}\vec{v}\right) = \eta\nabla^2\vec{v} - \frac{\eta}{\xi^2(\phi)}\vec{v} - \vec{\nabla}P \qquad (1)$$

where $\xi(\phi)$ corresponds to essentially the "mesh size" characterizing the local coiling (or "blobs") and is a function of the monomer density. The Brinkman equation was originally proposed to describe hydrodynamic flow in a porous medium with a typical pore size, ξ. If the interface between the porous medium and the pure fluid is very sharp, the flow of the fluid outside the medium only penetrates into the medium to a certain depth, the hydrodynamic penetration length, which is essentially the pore size, ξ. Therefore, the term $-\eta/\xi^2(\phi)\vec{v}$ in eq 1 represents such an attenuation effect. In using the Brinkman equation as a description of the hydrodynamics of the solvent inside the brush region, we make the simplest approximation that the brush region behaves as a porous medium with the "pore size" being a local quantity that depends on the "time-averaged" local monomer density.[21] The effective hydrodynamic penetration length in this case is, therefore, strongly affected by the details of the monomer density profile, as pointed out by Milner:[19] A parabolic density profile, as the SCF theory predicted, leads to a much greater penetration into the brush region of the flow of solvent than a step-function density profile would allow. This interesting observation makes our consideration of the effect of the hydrodynamic flow inside the brush region very meaningful, especially when our simulation provides a more detailed and realistic density profile than the parabolic one; we may expect that the exponential tail in the density profile enhances the penetration even more.

The response of a polymer brush to a shear flow of its solvent in the direction parallel to the grafting surface, as revealed by our simulation, can be summarized qualitatively as follows: The hydrodynamic flow of the solvent does have a very significant penetration into the brush region, and the polymer molecules respond to the flow by adopting configurations that show, on average, both net tilting toward the flow direction and stretching beyond the linear dimension the molecules assume when the solvent flow is absent. These changes in polymer configurations and the underlying mechanism can be understood in terms of a

very simple macroscopic picture, as depicted in Figure 1b. In a brush that is in equilibrium with a static solvent, the stretching of the polymer molecules is *normal* to the grafting surface, and it can be macroscopically described as the result of the balance between two forces that are both normal to the grafting surface: the osmotic pressure inside the brush (a macroscopic manifestation of the interaction between the polymer and its solvent) and the elastic restoring force of the brush (also a macroscopic description of the tendency of the polymer to maximize its configurational entropy). As the flow of the solvent is turned on, it effectively exerts a force on the brush that is parallel to the grafting surface. In order to offset this extra force, the molecules tilt toward the flow direction and also stretch themselves further out than they do in the former case.

Recently, in a very interesting paper, Lai and Binder have computed the properties of polymer brushes under shear, using a bond-fluctuation lattice Monte-Carlo model.[11] In their calculation the flow was also modeled by the Brinkman equation, while the polymer brush profile was assumed to be a parabolic shape as determined by SCF theory with the brush height determined iteratively. In particular they have focused on the scaling behavior of the polymer brush under shear. Their simulation indicated that the density profile and the distribution for the perpendicular coordinate, z_N, of the free ends differ very little whether there is shear or not; on the other hand the distribution of the free-end coordinates parallel to the flow is strongly influenced by the shear. Our results (see below) are in good agreement with these findings insofar as the comparison is possible, although our simulations are based on a different algorithm. Moreover, since our algorithm allows us to tackle systems with much larger numbers of degrees of freedom, we are able to carry out our calculation using a self-consistently determined density profile rather than the assumed parabolic one. As it is well known that the parabolic density profile determined in the SCF theory does not agree with those obtained by Monte-Carlo or molecular dynamics simulations in the tail region—large fluctuations that are properly represented in simulations cause the density to decay exponentially to zero—and also as the shear flow penetrates the brush through the tail region, it is important to model this region as realistically as possible. Furthermore, we analyze semiquantitatively the observed chain tilting and stretching in the framework of a macroscopic theory proposed by Rabin and Alexander.[10] Our analysis and the fact that our numerical data are largely consistent with the result of their phenomenological calculations provide more microscopic insights into the phenomenological theory and its underlying physics.

The plan of the paper is as follows. Section 2 gives an account of the numerical method used in our study, including the recapitulation from ref 6 of the model Hamiltonian and some of the description of the off-lattice simulation method, insofar as they are needed here. Section 3 represents the numerical results and our analysis of the results. Section 4 ends the paper with a brief discussion on the connection of our simulation study to some recent experiments on sheared polymer brushes.

2. Model Formulation and Numerical Method

Following ref 6, we use the Edwards Hamiltonian to describe a polymer brush, which consists of K monodispersed chains, each having $N + 1$ monomers with $n = 0$ as the grafted end. Let $\mathbf{r}_i(n)$ represent the spatial position of the nth monomer located on the ith polymer. The Hamiltonian, in the continuum limit ($N \to \infty$), is written as follows:

$$\frac{H\{\mathbf{r}_i(n)\}}{k_B T} = \frac{1}{2}\sum_{i=1}^{K}\int_0^N \mathrm{d}n\left(\frac{\mathrm{d}\mathbf{r}_i(n)}{\mathrm{d}n}\right)^2 + \nu\{\mathbf{r}_i(n)\} \tag{2}$$

The first term is the sum of Gaussian stretching of all bonds between neighboring monomers on the same chain. $\nu\{\mathbf{r}_i(n)\}$ describes the short-range interactions between monomers. In the case of polymers mixed with a good solvent, ν is well approximated by the second term in the virial expansion of the interaction energy and often referred to as "excluded-volume interaction" in literature; it is given by

$$\nu\{\mathbf{r}_i(n)\} = \frac{1}{2}w_2\int \mathrm{d}\mathbf{r}\phi^2(\mathbf{r}) \tag{3}$$

where w_2 is positive, characterizing the good solvent. $\phi(\mathbf{r})$ is the local concentration of monomers which can be written as

$$\phi(\mathbf{r}) = \sum_{i=1}^{K}\int_0^N \mathrm{d}n\ \delta(\mathbf{r} - \mathbf{r}_i(n)) \tag{4}$$

For our simulations, we use $w_2 = {}^1/_2$.

In our simulations, microscopic configurations of the brush are described by the spatial positions of the individual monomers; the basic constraints are that one end of each polymer chain is grafted at a random position on the substrate, represented by the xy-plane at $z = 0$, and the other monomers lie in the upper half-space ($z \geq 0$). To calculate the energy for each configuration, the integrations in the Hamiltonian given in eq 2 are replaced by summations: The Gaussian stretching term is then

$$\frac{1}{2}\sum_{i=1}^{K}\sum_{n=1}^{N}[\mathbf{r}_i(n) - \mathbf{r}_i(n-1)]^2 \tag{5}$$

and the excluded volume interaction energy is obtained by dividing the system into a fine grid of cubic boxes, counting the number of monomers in each box to find the coarse-grained local monomer density, and summing the contributions from all the boxes, *i.e.*,

$$\nu\{\mathbf{r}_i(n)\} = \frac{1}{2}w_2\sum_{k=1}^{N_{\mathrm{box}}} V_{\mathrm{box}}\phi^2(k) \tag{6}$$

where N_{box} is the total number of the boxes used for coarse graining, V_{box} is the volume of each box, and $\phi(k)$ is the monomer density in box k.

To describe the hydrodynamic flow of the solvent, we consider the following situation. Imagine that there is another solid surface at distance L from the substrate and it moves parallel to the substrate with a velocity of v_0. In the absence of a polymer brush, this creates a simple shear flow in the solvent filling the space between the two surfaces, $v(z) = \gamma z$, where $\gamma \equiv v_0/L$ is called shear rate. The presence of a brush end-grafted onto the substrate changes the flow profile, as we have briefly discussed in the Introduction; in this case, a simple shear flow in its steady state is determined by the following equations:

$$\frac{\mathrm{d}^2 v_1}{\mathrm{d}z^2} = 0,\ h < z < L$$

$$\frac{\mathrm{d}^2 v_2}{\mathrm{d}z^2} = \frac{v_2}{\xi^2(\phi)},\ 0 \leq z \leq h \tag{7}$$

subject to the boundary conditions,

$$v_1(L) = \gamma L \text{ and } v_2(0) = 0 \tag{8}$$

and the conditions for continuity of the velocity profile at the brush−solvent interface $z = h$,[22]

$$v_1(h) = v_2(h) \text{ and } \frac{dv_1}{dz}|_{z=h} = \frac{dv_2}{dz}|_{z=h} \tag{9}$$

The second equation in eq 7 is just a simple case of the Brinkman equation (eq 1).

The length scale ξ in eq 7 is essentially the hydrodynamic screening length. For a semidilute polymer solution in a good solvent, it is of the same order as the "mesh" size, l_M. de Gennes, using scaling arguments, has shown that l_M scales as $a\phi^{-3/4}$,[17] where a is of the order of the monomer size and ϕ is the volume fraction of the polymer. We assume the same scaling behavior, *i.e.*, $\xi(\phi) \sim \phi^{-3/4}$, for the dense polymer brushes under our consideration, which have polymer concentrations that are typical of semidilute solutions. A simple scaling argument based on an idealized picture proposed also by de Gennes for dense polymer brushes[23,24] leads to this scaling behavior.

Equation 7 is a nonlinear equation for $v(z)$, since the hydrodynamic screening length, $\xi(\phi)$, has an implicit nonlinear dependence on $v(z)$ through the local monomer density, $\phi(z)$. The main task of the numerical study of the problem is to solve this nonlinear equation for $v(z)$ and, in turn, $\phi(z)$, and the solution is found by using the following iteration procedure: An initial monomer density profile is used to find the corresponding velocity profile by solving eq 7; the velocity profile is then used to find a new monomer density profile through a Monte-Carlo simulation of the brush; the new density profile is in turn used as the new input for solving eq 7 again. The iteration proceeds until a specified self-consistency criterion is satisfied.

The simulations are carried out using an algorithm that is based on the standard Metropolis Monte-Carlo procedure but contains modification to take into account the effect of a solvent flow (in the x-direction) in the brush region. As described in the Introduction, the impact of the solvent flow is modeled in our Monte-Carlo procedure by an enhanced transition probility of a monomer to move in the flow ($+x$) direction. Specifically, the effective transition rate from a state, $S = \{x_i(n), y_i(n), z_i(n); i = 1, K; n = 1, N\}$, to a new state, $S' = \{x_i'(n), y_i'(n), z_i'(n); i = 1, K; n = 1, N\}$, is given by

$$W(S, S') = D_0(S, S')\{1 + \mu\sum_{k=1}^{K}\sum_{n=1}^{N} v(z_i(n))[x_i'(n) - x_i(n)]\} \exp\left(-\frac{1}{2}[E(S') - E(S)]/k_BT\right) \tag{10}$$

$D_0(S, S')$ is chosen to be symmetric, *i.e.*, $D_0(S, S') = D_0(S', S)$, and is nonzero only if S and S' are "nearby" states, *i.e.*, $|S' - S| < \Delta$, where Δ is some specified value. The expression enclosed in the curly bracket represents the asymmetric jumping rates; the parameter μ plays the role of the "friction coefficient" and takes small values in our simulations. An attempted random move of a monomer is therefore either accepted or rejected according to the transition rate calculated from (10). In this algorithm, the connectivity of a chain is automatically ensured by the Gaussian stretching term in the Hamiltonian (2): Moving two neighboring monomers too far apart costs a large amount of energy; hence, any configurations of this type will be rejected. With the modified transition rate, eq 10, the configurations of the brush subject to a particular solvent flow with velocity profile $v(z)$ can be simulated, and its statistical properties, including the averaged local monomer density, can be obtained and analyzed.

An important remark is in order here. The transition probability (10) in general does not satisfy detailed balance. However, with a judiciously chosen $D_0(S, S')$, as described above, for which the condition $v(z_i'(n)) \cong v(z_i(n))$ holds, it can be shown that the detailed balance is observed when μ is small. Hence, a new "equilibrium" state of the brush under the influence of a solvent flow can be reached after a sufficient number of Monte-Carlo steps. We typically use 5×10^5−10^6 Monte-Carlo steps per monomer during each simulation run, including those steps used for the "equilibration" of the system.

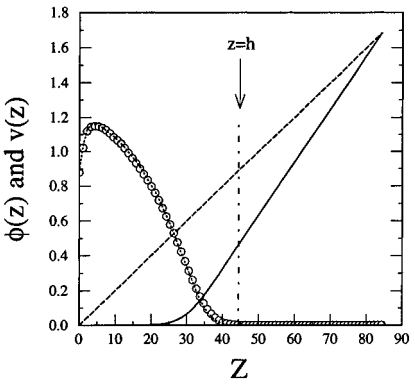

Figure 2. Interplay between a polymer brush and a shear flow of its solvent. Velocity profile $v(z)$ of the solvent in the presence of the brush is shown by the solid curve; the simple shear flow of the pure solvent is drawn in the dashed line for comparison, to emphasize the screening effect of the brush on the solvent flow. Monomer density profiles, for both $\gamma = 0$ (dotted curve) and $\gamma \neq 0$ (○), are also given. Their magnitude has been scaled for visual purpose.

3. Results: Chain Tilting and Stretching

The screening effect of the polymer brush on the hydrodynamic flow of the solvent is clearly seen in Figure 2, where a typical velocity profile is plotted, in comparison with the monomer density profile. Outside the brush region $h < z < L$, where the monomer density is zero, the velocity profile is that of a simple shear flow, $v(z) = v_0 + \gamma'(z - L)$; however, due to the presence of the brush, the slope of this linear profile, γ', is larger than the shear rate, defined as $\gamma \equiv v_0/L$. Inside the brush, the flow is attenuated because of the screening but with a substantial depth of penetration.

In contrast, the equilibrium monomer density of the brush shows very little sensitivity to the hydrodynamic flow, as also shown in Figure 2, *although* the conformation of each individual polymer chain in the brush is strongly perturbed by the penetrated flow, as we will discuss in the following text.

Figure 3 is a collection of some of the instantaneous configurations of the polymer chains in the brush in equilibrium with the external force due to the solvent flow for two different shear rates. Qualitatively shown in these snapshots is that the chains, in response to the flow, tilt away from the normal of the substrate and toward the direction of the flow and the extent of the tilting increases as the shear rate increases. Quantitatively, this tilting can be characterized by the following geometric parameter:

$$\cos\theta = \hat{R}_{CM} \cdot \hat{x} \tag{11}$$

where $\hat{R}_{CM}$ is the unit vector pointing to the center of mass of a chain from its grafted end and $\hat{x}$ is the unit vector in x-direction; θ, the angle between the two unit vectors, measures the extent of the inclination. Figure 4 is a plot of $\langle\cos\theta\rangle$ as a function of γ, for a fixed chain length ($N = 100$) and a fixed grafting density ($\sigma = 0.1$). $\langle\cos\theta\rangle$ indeed increases as the shear rate is raised, indicating a γ-dependent tilting of the molecules away from the direction normal to the surface.

As we briefly pointed out in the Introduction, the balance of the different forces—the elastic restoring

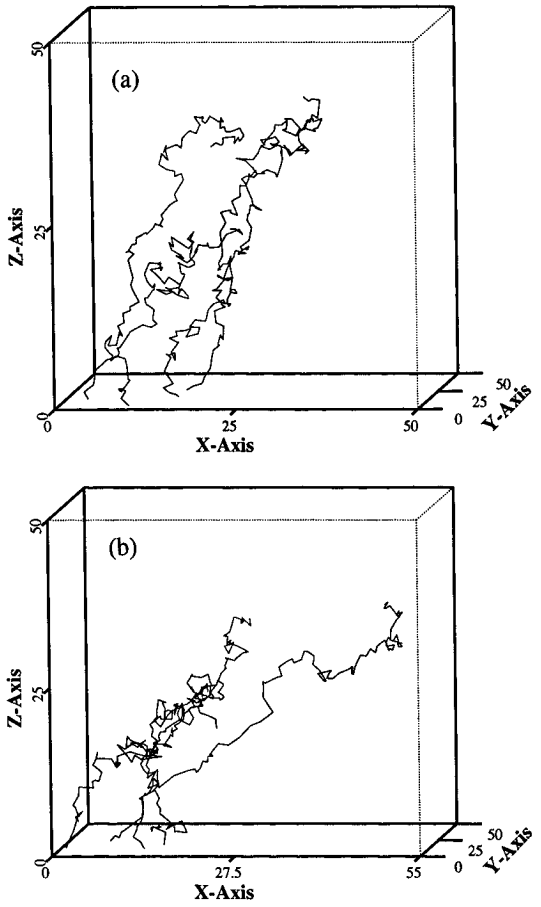

Figure 3. Instantaneous configurations of the polymer chains in a brush under shear: (a and b) two different shear rates, γ = 0.005 and 0.01, respectively. The increase with γ in both the tilting and stretching of the chains is apparent. For clarity, only four chains are displayed out of 100. Each chain has 100 monomers, and the grafting density is 0.1.

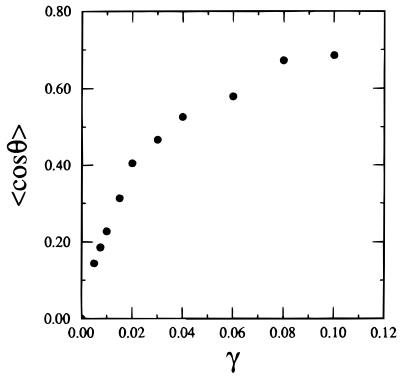

Figure 4. <cos θ> vs γ. The tilting of the chains in the flow direction is quantitatively characterized.

force, the osmotic pressure, and the force arising from the solvent flow—requires not only the tilting of the chains but also their stretching. Several quantities, corresponding to different ways of characterizing the linear dimensions of the chains, serve as different measures of the stretching. The most natural one is the average position of each monomer on a single chain, with respect to the anchored end of the chain. Figure 5a displays such averaged molecular shapes by showing $\langle z(n)\rangle$ as a function of $\langle x(n)\rangle$, for a series of values of the shear rate. While $\langle z(n)\rangle$ remains essentially unchanged as the shear rate increases, $\langle x(n)\rangle$ increases approximately linearly with γ, a clear evidence of the overall extension in the linear dimension of the chains. The

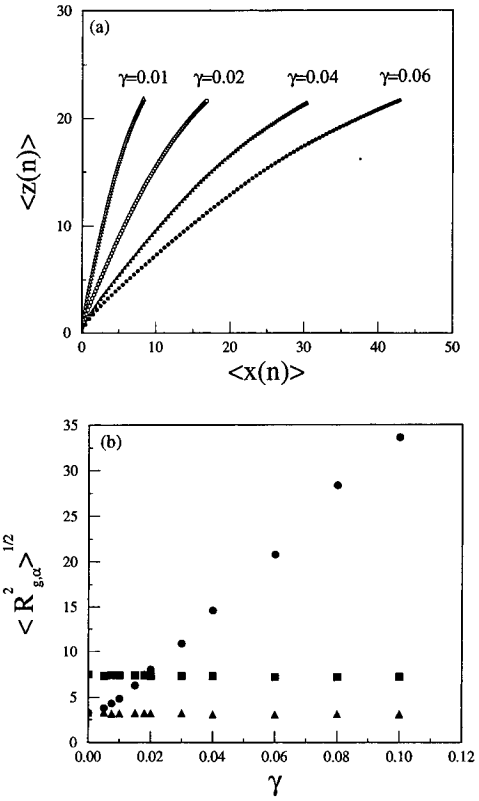

Figure 5. Stretching of polymer chains by solvent shear flow. (a) Chain conformation on average is shown for four different shear rates; the stretching is seen in the increased linear dimension of the chains. (b) x (●), y (▲), and z (■) components of the radius of gyration (R_g) are given as functions of γ. The stretching manifests itself principally in the x component.

same stretching is also indicated by the response to the flow of the x,y,z components of the radius of gyration,

$$\langle R^2_{g,\alpha}\rangle \equiv \left\langle \frac{1}{N+1}\sum_{n=0}^{N}[r_\alpha(n) - R_{CM,\alpha}]^2 \right\rangle \qquad (12)$$

where $\alpha = x,y,z$ and $\vec{R}_{CM}$ is the position of the center of mass of the chain, and by the response of the end-to-end distance

$$\langle R_e\rangle^2 \equiv \langle \vec{r}(N) - \vec{r}(0)\rangle^2 \qquad (13)$$

In Figure 5b, $\langle R^2_{g,\alpha}\rangle^{1/2}$ and $\alpha = x,y,z$, are shown as functions of γ. Again, it can be seen that the linear dimensions of the chains in both the y- and z-directions stay practically constant across the range of the shear rates that we have explored, whereas the molecular span in the x-direction is increased with the shear rate, leading to an overall stretching of the chains, as also indicated by the increase of $\langle R_e\rangle$ with γ. The functional dependence on γ of $\langle R^2_{g,\alpha}\rangle^{1/2}$ will be discussed in detail in later text.

It is natural at this point to ask how the stretching of the polymer chains that we have observed in our simulation takes place at the microscopic level, even though the physics underlying the stretching are easily understood at the macroscopic level, as discussed in section 1. The answer lies in the substantial coiling at short-length scales that is present in the conformation of the chains when there is no flow in the solvent (see section 1). The evidence of this local coiling is provided unambiguously by the simulations:[6] The average linear span of each molecule is only about 10% of its fully

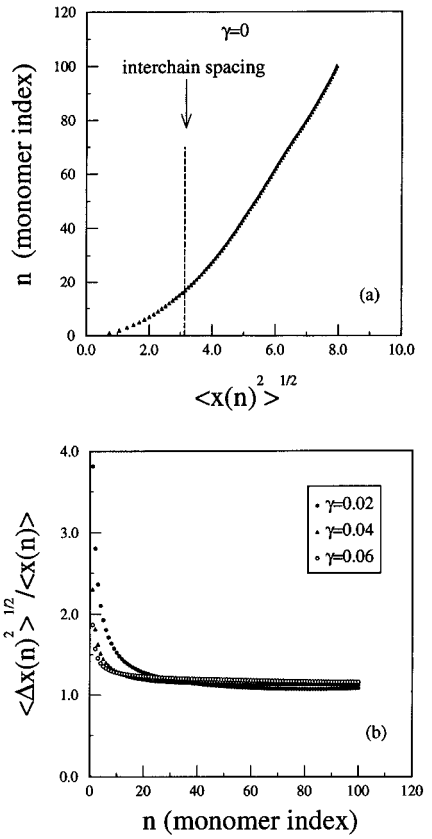

Figure 6. Fluctuations in monomer positions in the x-direction: (a and b) $\gamma = 0$ and three different values of γ, respectively. Fluctuations are already larger than the interchain spacing, $\sigma^{-1/2}$, in case a; they are enhanced in the presence of solvent shear flow.

stretched length, and the monomer density becomes essentially zero beyond a distance (from the substrate) that is only one-fourth of the full molecular length. The effect of the solvent flow is to unwind these local coils and align the chains as much as possible in the direction of the solvent flow. The earlier study of Lai and Binder[11] has shown that the segments on each individual chain exhibit a greater alignment along the mean direction of the chain in the presence of the solvent flow.

Another interesting and important question concerns the configurational fluctuations of the stretched polymer chains. One might think that (strongly) stretched chains resemble rigid rods and thus would have transverse fluctuations comparable to monomer (or "blob") size; in a brush, such fluctuations would then be of the order of $\sigma^{-1/2}$, the interchain spacing. However, it actually turns out that, in a brush in equilibrium with a static solvent, the transverse excursions of the chains already take place on length scales larger than the interchain spacing; they become even larger when the chains are stretched more by "external" forces, as shown in Figure 6. Figure 6a illustrates for the case where $\gamma = 0$ the excursion in the x-direction of each monomer away from its equilibrium position, $\langle x(n)\rangle = 0$; the transverse movement of those monomers that are closer to the free end of the chain is certainly substantial, being a few times larger than $\sigma^{-1/2}$. Figure 6b is a plot of $\langle[x(n) - \langle x(n)\rangle]^2\rangle/\langle x(n)\rangle^2$ as a function of n, for nonzero values of γ, showing much greater excursions of the monomers in the x-direction. This phenomenon is not difficult to rationalize; as suggested by Rabin *et al.*,[10] the stretching of each chain leads to more fluctuations in the local monomer density within the free volume of the chain, or simply put, there is more free space for monomers from the neighboring chains to make their excursion to. What this amounts to is an effective reduction in the excluded volume of each individual chain, thereby stronger fluctuations in monomer positions. This revelation of the enhanced fluctuations in the sheared brush by the simulation provides a microscopic basis for the suggestion which is embodied in the estimate of the osmotic force, eq 15 (see below).

The stretching of the chains as a consequence of the balance of the different forces involved, as depicted in Figure 1, can be further analyzed in a semiquantitative fashion. Rabin *et al.* have developed a macroscopic theory to describe the stretching.[10] In their theory, the elastic restoring force is assumed to take the nonlinear expression originally proposed by Pincus:[25]

$$F_{el} = \frac{k_B T}{b}\left(\frac{R_e}{Nb}\right)^{3/2} \tag{14}$$

where R_e is the linear extension of the chain, well represented by the end-to-end distance which we have directly "measured" in our simulations. The osmotic pressure is estimated to be

$$F_{osm} = k_B T \sigma b \frac{(R_e/Nb)^{1/2}}{(h/Nb)^2} \tag{15}$$

where $h = R_e \sin\theta$. This expression for the osmotic pressure is different from the usual form used for a semidilute polymer solution,[17] reflecting the enhanced local monomer density fluctuations due to the chain stretching. The force balance can thus be formulated as

$$F_{osm} = F_{el} \sin\theta$$
$$F_{shear} = F_{el} \cos\theta \tag{16}$$

The solution to this set of equations is the following:

$$\frac{h}{R_e(0)} \cong 1 \tag{17}$$

and for $F_{shear} \ll 1$,

$$\frac{R_e}{R_e(0)} \cong 1 + C_0 F_{shear}^2 \tag{18}$$

whereas for $F_{shear} \gg 1$,

$$\frac{R_e}{R_e(0)} \cong C_1 F_{shear}^{2/3} \tag{19}$$

$R_e(0)$ is the average end-to-end distance when the shear force is zero; C_0 and C_1 are just constants for a fixed grafting density. Equation 17 predicts that the height of the polymer shows no response to the shear flow, which is in accord with our finding through the simulation. More of our simulation results are presented in Figure 7 where the functional dependence of $R_e/R_e(0)$ on γ is displayed in two different manners, corresponding to those proposed by the theory for the two different regimes of the shear rate, respectively. For small values of γ, Figure 7a shows $R_e/R_e(0)$ as a linear function of γ^2, which fits very well with eq 18. For larger values of γ, Figure 7b is a log−log plot of R_e vs γ to give a better perception of the possible power law behavior suggested

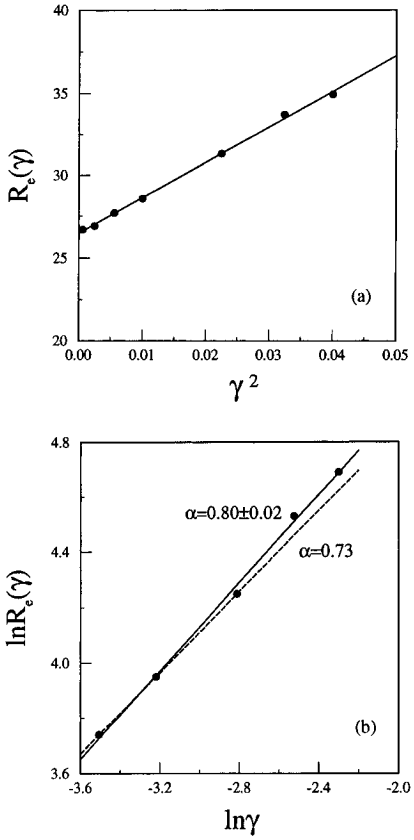

Figure 7. Two different regimes of scaling with γ of the stretching characterized by the chain end-to-end distance, R_e: (a) a low-shear regime, where R_e is linear in γ^2, and (b) a high-shear regime, where R_e scales with γ in a power law behavior. Simulation data is shown in solid circles, and the solid and dashed lines show two linear fits of the data, corresponding to two different fitting ranges. These two fits yield slightly different exponents for the power law scaling. Simulation results are in good agreement with the theory proposed by Rabin *et al.*,[10] which predicts an exponent of $^2/_3$.

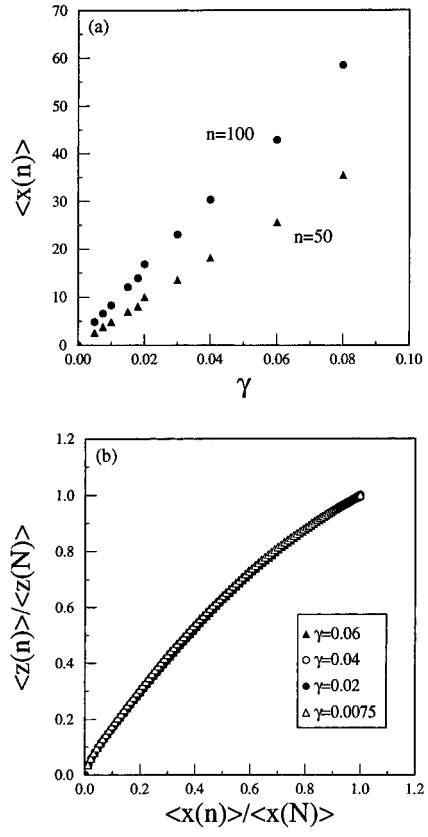

Figure 8. Linear dependence on γ of averaged molecular trajectories: (a) the averaged positions in the x-direction of two different monomers, $n = 50$ and 100 (the free end), and (b) the "normalized" trajectories for four different shear rates. The collapse of the data onto a single curve demonstrates unambiguously the scaling described by eq 20.

by eq 19; indeed, a power law behavior is observed, but the exponent obtained from the fitting is slightly larger than $^2/_3$, ranging from 0.73 to 0.80 (see below). Here, we have implied our observation that F_{shear} is proportional to γ.[26] Figure 7 suggests that our simulation results compare rather well with the theory of Rabin *et al.* for stretched polymer brushes.[10] Our simulation study provides strong support both to the claim that the stretching proceeds within the nonlinear regime of polymer elasticity[25] and to the scaling form (eq 15) proposed for the osmotic pressure inside a stretched grafted polymer layer,[10] at least when the linear extension of the chains, stretched as they are, is still significantly shorter than that of a fully-stretched chain.

It is useful to make two remarks on the analysis we have just described. The first is on the applicability of the nonlinear force law to our situation. It is well established that the nonlinear force law has its origin in the excluded-volume interaction between monomers from the same chain ("self-avoidance") and is only valid in the particular regime where the chain linear extension is much larger than its radius of gyration in free solution but much smaller than its fully-extended length. We believe that for the shear rate values that we have explored, we operate mainly in this regime. However, in cases where the chains are stretched to a length that is close to its fully-extended dimension, the excluded-volume interaction between monomers from the same chain is effectively removed; consequently, the stretching will cross over to the linear regime within our description of the chains, for the Edwards Hamiltonian assumes Gaussian stretching behavior in the absence of self-avoidance. This crossover may account for the slightly higher (than $^2/_3$) power law exponents shown in Figure 7b for the higher shear rates. The second remark concerns eq 16. As Barrat has pointed out,[27] there should in principle be another force in the direction parallel to the shear force, corresponding to the fluctuations of the molecular trajectory about its mean-field path given by eq 16. Therefore, the true path, as obtained from the simulation, may deviate away from the mean-field path. However, we believe that this effect will be small: It has to diminish as the system approaches the unsheared limit; it provides only a small correction when the chains are strained significantly by the shear force, seen from the estimate given in ref 27. More importantly, the scaling behavior we have observed in our simulation data will not be altered by this small correction.

We end this section with a final remark on the dependence on the shear rate of the mean trajectory of the chains. The increase with the shear rate of the average monomer positions, as mentioned in the previous text, is recapitulated in Figure 8a. Figure 8b displays the "normalized" molecular trajectories, $\langle z(n)\rangle/\langle z(N)\rangle$ vs $\langle x(n)\rangle/\langle x(N)\rangle$, for a few different values of the shear rate, γ. It is apparent that these "normalized" trajectories are almost independent of γ. Again, this result can be easily understood on the basis of the notion of the force balance, but considered from the perspective of each individual monomer. At equilibrium, the elastic "spring" force in the x-direction (due to Gaussian

stretching) acting on a monomer by its neighboring monomers must be balanced by the shear force, *i.e.*,[28]

$$\frac{\partial^2\langle x(n)\rangle}{\partial n^2} \cong \gamma\, \mathrm{f}(\langle z(n)\rangle) \tag{20}$$

where $f(\langle z(n)\rangle)$ is essentially the function, $v(z(n))/\gamma$, which has no significant dependence on γ. It is straightforward to see that Figure 8 is simply an illustration of eq 20.

4. Discussion

In summary, we have studied the properties of a polymer brush in equilibrium with a solvent that is subject to a shear flow. The interplay between the polymer brush and the hydrodynamic flow of the solvent has been modeled, with simple but largely justifiable approximations. The main technique used in our study is a Monte-Carlo simulation algorithm that is distinct from many standard numerical methods used in studies of polymer brushes, in that it combines an off-lattice description of polymer brushes—the Edwards Hamiltonian—with a modification of the standard Metropolis MC transition probability to take into account the effective force acting upon the polymer molecules by the moving solvent. The conformation of the polymer brush, the configurations of each individual chain in particular, is investigated in detail. It is found that the significant response of the brush to the solvent shear flow manifests principally in the form of the chain tilting toward and stretching along the direction of the flow, whereas the overall conformational properties, such as the averaged local monomer density, and the linear span of the brush in the direction normal to that of the flow remain essentially unaffected by the flow. Such response can be understood both qualitatively and semiquantitatively in terms of a notion of the mechanical balance of the different physical forces involved, which was used in the recent theory of Rabin and Alexander. We also note that our simulation results are entirely consistent with those obtained in an earlier study of Lai and Binder, insofar as the comparison can be done, although they have used the bond-fluctuation algorithm to simulate polymer configurations.

It is natural that we, having borne in mind the fact that experiments have been performed to study polymer brushes under shear,[9] ask the following question: How relevant is the physics we have modeled to that underlying the experimental findings? The experiments of Klein *et al.*[9] measure the normal force between two polymer brushes that are sheared against each other. It is observed that, once the shear rate reaches a threshold value, a strong repulsion sets in between the brushes even when they are at a distance where there is no force in the absence of the shear. This shear-induced repulsion is interpreted as an increase in the brush height. Apparently, neither the analytical (mean-field type) calculation of Rabin *et al.*[10] nor our numerical simulation (nor, as a matter of fact, that of Lai and Binder[11]) provides an explanation for such an increase in the brush height.

It is not clear at this stage what is truly the origin of this apparent discrepancy between theory and experiment.[29] We close this discussion by pointing out at least possible mechanisms that may underly the disagreement. One possibility is that the increase of the brush thickness may be due to substrate corrugation, which is likely to exist in experimental systems but certainly has not been considered in all the theoretical modeling. The possible surface irregularity would inevitably induce a velocity component in the direction normal to the surfaces. Within the framework of our modeling, such a velocity component (if positive) is expected to lead to an increase in the brush thickness. This possibility has been proposed and discussed in refs 11, 30, and 31.

Another interesting possibility was raised by Kumaran.[32] The hydrodynamic perturbation of a polymer brush on the flow of the solvent inside the brush is analyzed for the case where the brush has a *finite* extent on the substrate. In this case, the tilting of the brush creates an asymmetry in the pair distribution of monomers, which tends to cause a net flow of the solvent in the direction normal to the substrate. To suppress this flow in the normal direction, the brush has to exert a downward force on the solvent, and vice versa, the solvent has to react with an upward force on the brush. This upward force may cause the brush to swell. The description of a brush of finite extent may be a more realistic one of the experimental situation than that used in our simulations, which corresponds to a brush of an *infinite* extent.

One could also ask if what has been observed in the experiment is rather a dynamic effect. It can easily be argued that the internal relaxation time of polymer molecules—the longest Rouse relaxation time—is much shorter than the time scale set by the shear rate and the frequency of the surface oscillations in the experiment. On the other hand, the relaxation dynamics of each molecule as a whole may be slower. However, there is no sufficient amount of study done in this respect for one even to make order-of-magnitude estimates.

Acknowledgment. H.G. thanks Prof. P. Y. Lai for a useful discussion. We gratefully acknowledge support from the Natural Sciences and Engineering Research Council of Canada and le Fonds pour la Formation de Chercheurs et l'Aide à la Recherche de la Province du Québec. Finally, we would like to express our sincere gratitude to Prof. Y. Rabin for bringing to our attention the work reported in ref 32.

References and Notes

(1) Napper, D. *Polymer Stabilization of Colloidal Dispersions*; Academic Press: London, 1983.
(2) Wu, S. *Polymer Interfaces and Adhesion*; M. Dekker: New York, 1982.
(3) de Gennes, P.-G. *J. Phys. (Paris)* **1976**, *37*, 1443; *Macromolecules* **1980**, *13*, 1069.
(4) Milner, S. T.; Witten, T. A.; Cates, M. E. *Europhys. Lett.* **1988**, *5*, 413; *Macromolecules* **1988**, *21*, 2610.
(5) Murat, M.; Grest, G. S. *Phys. Rev. Lett.* **1989**, *63*, 1074.
(6) Laradji, M.; Guo, H.; Zuckermann, M. J. *Phys. Rev. E* **1994**, *49*, 3199.
(7) Taunton, H. J.; Toprakcioglu, C.; Klein, J. *Macromolecules* **1988**, *21*, 3336. Taunton, H. J.; Toprakcioglu, C.; Fetters, L. J.; Klein, J. *Nature (London)* **1988**, *332*, 712; *Macromolecules* **1990**, *23*, 571.
(8) Milner, S. T. *Science* **1991**, *251*, 905. Halperin, A.; Tirrell, M.; Lodge, T. P. *Adv. Polym. Sci.* **1991**, *100*, 31.
(9) Klein, J.; Perahia, D.; Warburg, S. *Nature* **1991**, *352*, 143.
(10) Rabin, Y.; Alexander, S. *Europhys. Lett.* **1990**, *13*, 49.
(11) Lai, P.-Y.; Binder, K. *J. Chem. Phys.* **1993**, *98*, 2366.
(12) An example of the effect of fluctuations is the appearance of an exponential tail in the monomer density profile of a brush of polymers of finite chain length. This exponential tail is particularly important to the study of the forces between two brushes of short chains.
(13) Katz, S.; Lebowitz, J. L.; Spohn, H. *Phys. Rev. B* **1983**, *28*, 1655; *J. Stat. Phys.* **1984**, *34*, 497.
(14) Kirkwood, J. G.; Riseman, J. *J. Chem. Phys.* **1948**, *16*, 565.

(15) Zimm, B. H. *J. Chem. Phys.* **1956**, *24*, 269.
(16) Doi, M.; Edwards, S. F. *The Theory of Polymer Dynamics*; Oxford University Press: New York, 1986.
(17) de Gennes, P.-G. *Scaling Concepts in Polymer Physics*; Cornell University Press: Ithaca, NY, 1979.
(18) Richter, D.; Binder, K.; Ewen, B.; Stühn, B. *J. Phys. Chem.* **1984**, *88*, 6618.
(19) Milner, S. T. *Macromolecules* **1991**, *24*, 3704.
(20) Brinkman, H. C. *Appl. Sci. Res.* **1947**, *A1*, 27.
(21) By using the averaged local monomer density, we implicitly make the assumption that the time scale at which the monomer density fluctuates is much shorter than the time scales typical for the macroscopic flow of the solvent.
(22) h is defined to be the distance from the substrate at which the monomer density becomes zero. We also note that one of the conditions for velocity continuity at the brush−solvent interface, $dv_1/dz|_{z=h} = dv_2/dz|_{z=h}$, eliminates the "kink" that appeared in the velocity profile calculated in ref 11. This condition is correct, since a "kink", or the discontinuity, in the first derivative of the velocity would imply a singular viscous force acting upon the fluid elements at the interface.
(23) de Gennes, P.-G. *Adv. Colloid Interface Sci.* **1987**, *27*, 189.
(24) The picture that leads to this scaling for the brushes is the following: Each chain is described as a sequence of subunits, called "blobs", and each blob is characterized by the swelling exponent $\nu = {}^3/_5$. Of course, it should be kept in mind that a brush formed from polymer molecules of finite chain length deviates to some extent from this picture. It should also be noted that, when chains are stretched by very strong forces, as may be the case when the shear flow is strong, the blob size is determined by the stretching force.
(25) Pincus, P. *Macromolecules* **1976**, *9*, 386.
(26) That F_{shear} is linear in γ does not hold in general, for eq 7 is, strictly speaking, a nonlinear differential equation in v. However, as we have observed, the averaged monomer density, ϕ, and, in turn, the hydrodynamic screening length, $\xi(\phi)$, do not depend on the velocity profile; eq 7 thus becomes practically linear, and its solution, $v(z)$, is therefore linear in v_0 or γ. Consequently, the shear force, F_{shear}, is linear in γ.
(27) Barrat, J.-L. *Macromolecules* **1992**, *25*, 832.
(28) In this approximation, the effect of the excluded-volume interaction is being neglected.
(29) Barrat discussed a mechanism in ref 27 for swelling of a brush under shear. However, it can be shown that the "brush swelling" predicted there is an artifact due to an underestimate of the brush thickness in the limiting case of zero shear (Ling Miao, unpublished results).
(30) Atkinson, J.; Goh, C. J.; Phan-Thien, N. *J. Chem. Phys.* **1984**, *80*, 6305.
(31) Bagassi, M.; Chauveteau, G.; Lecourtier, J. *Macromolecules* **1989**, *22*, 262.
(32) Kumaran, V. *Macromolecules* **1993**, *26*, 2464.

MA951071Z